International Journal of Automotive Technology, Vol. 7, No. 6, pp. 729–739 (2006)

1229-9138/2006/030-12

ACTIVE FAULT-TOLERANT CONTROL OF INDUCTION MOTOR DRIVES IN EV AND HEV AGAINST SENSOR FAILURES USING A FUZZY DECISION SYSTEM

M. E. H. BENBOUZID[1)*], D. DIALLO[2)], M. ZERAOULIA[1)] and F. ZIDANI[3)]

[1)]Laboratoire d'Ingénierie Mécanique et Electrique (LIME), IUT of Brest, University of Western Brittany, Rue de Kergoat–BP 93169, 29231 Brest Cedex 3, France
[2)]Laboratoire de Génie Electrique de Paris (LGEP) CNRS UMR 8507 Supélec, Plateau du Moulon, Paris XI, 91192 Gif-Sur-Yvette, France
[3)]LSPIE, University of Batna–1, Rue Chahid Boukhlouf, 05000 Batna, Algeria

(Received 26 September 2005; Revised 28 April 2006)

ABSTRACT–This paper describes an active fault-tolerant control system for an induction motor drive that propels an Electrical Vehicle (EV) or a Hybrid one (HEV). The proposed system adaptively reorganizes itself in the event of sensor loss or sensor recovery to sustain the best control performance given the complement of remaining sensors. Moreover, the developed system takes into account the controller transition smoothness in terms of speed and torque transients. In this paper which is the sequel of (Diallo *et al.*, 2004), we propose to introduce more advanced and intelligent control techniques to improve the global performance of the fault-tolerant drive for automotive applications (e.g. EVs or HEVs). In fact, two control techniques are chosen to illustrate the consistency of the proposed approach: *sliding mode* for encoder-based control; and *fuzzy logics* for sensorless control. Moreover, the system control reorganization is now managed by a fuzzy decision system to improve the transitions smoothness. Simulations tests, in terms of speed and torque responses, have been carried out on a 4-kW induction motor drive to evaluate the consistency and the performance of the proposed fault-tolerant control approach.

KEY WORDS : Automotive application, Induction motor drive, Fault-tolerant control, Sliding mode, Fuzzy logics

NOMENCLATURE

a, b	: fixed stator reference frame indexes
U_s (I_s)	: stator voltage (current)
ϕ_r (Ω)	: rotor flux (speed)
T_L	: load torque
f_s	: stator frequency
R_s (R_r)	: stator (rotor) resistance
L_s (L_r)	: stator (rotor) inductance
M	: mutual inductance
T_r	: rotor time constant, $T_r = L_r/R_r$
σ	: total leakage coefficient, $\sigma = 1 - M^2/L_sL_r$
n_p	: number of pole pair
J	: rotor inertia
J	: rotor inertia
f	: viscosity coefficient
γ	: constant, $\gamma = (R_s + M^2(R_r/L_r^2))/\sigma L_s$
K_L	: constant, $K_L = M/\sigma L_sL_r$
α	: constant, $\alpha = 1/\sigma L_s$
β	: constant, $\beta = n_pM/JL_r$
$\dot{x}$ ($\tilde{x}$)	: time derivative (complex) value
ref	: reference subscript
Δ	: variation term
meas	: measurement subscript
adj	: adjustment subscript
rat	: rated value subscript

*Corresponding author. e-mail: m.benbouzid@ieee.org

1. INTRODUCTION

The motor drive including the electric motor, the power converter, and the electronic controller is the core of the electric propulsion system in an EV or an HEV. As high reliability and maintenance-free operation are prime considerations in EVs and HEVs electric propulsion, adjustable speed ac motor drives are increasingly adopted in automotive applications to improve overall system efficiency and performance. This is the particular case of induction motor drives that are becoming attractive and considered as the most viable for modern EVs and HEVs. Indeed, the cage induction motor seems to be the candidate that better fulfils the major requirements of automotive electric traction (Zeraoulia *et al.*, 2005).

For the vehicle traction control, fault detection and

fault tolerance are important issues not only for the reliability of the drive system but also for the proper operation of the vehicle following a fault. In high impact automotive applications, such as EVs and HEVs, accept short torque transients and even permanently reduced drive performance after fault, on condition that the drive still goes running. Indeed, in these cases limp-back operation is preferred over no operation.

Induction motor drives control techniques are well treated in the literature. The most popular is the so-called scalar control method. This technique allows great performances only in steady state because precise control of the instantaneous torque is not possible. The vector control technique is now used for high impact automotive applications (EV and HEV). In this case, the torque control is extended to transient states and allows better dynamic performances (Lascu and Trzynadlowski, 2004; Mutoh *et al.*, 1997).

Depending upon the application and availability of sensors and the desired performance of the system, there are many hybrid schemes that could be combined for fault-tolerant purposes (Neacsu and Rajashekara, 2001). However, conventional linear control such as PID can no longer satisfy the stringent requirements placed on high performance EVs or HEVs. In recent years, many modern control strategies such as Model-Referencing Adaptive Control (MRAC), Self-Tuning Control (STC), Sliding Mode Control (SMC), Fuzzy Control (FC), and Neural Network Control (NNC) have been proposed (Chan, 2002). Both MRAC and STC have been successfully applied to EV propulsion (Chan *et al.*, 1990). Using sliding mode, SMC has also been applied to motor drives (Proca *et al.*, 2003). By employing emerging technologies of fuzzy and neural networks to realize the concept of intelligent controllers, NNC (Chen and Liu, 2003) and FC (Lee and Sul, 1998) have promising applications to EV and HEV propulsion. However, either fuzzy logic control or artificial neural network has its own drawbacks, which cannot be avoided and neglected. A simple fuzzy controller implemented in the motor drive speed control has a narrow speed operation and needs much manual adjusting by trial and error if high performance is wanted. On the other hand, it is extremely tough to create a serial of training data for neural networks that can handle all the operating modes. Neuro-Fuzzy Controllers (NFC), which has advantages of both FC and NNC are therefore adopted in some cases for induction motor control (Bose *et al.*, 1997).

Furthermore, automotive application drives such as in EV and HEV have some major requirements that are listed in (Rahman *et al.*, 2000). The main requirement that is related to the electric propulsion control is the ability to operate at constant power over a wide speed range, good overload performance, and high efficiency, especially at light load operation at higher speeds. These characteristics allow the best utilization of the limited battery capacity (extension of the running distance per battery charge) and the minimization of the size and the weight of the motor and the drive. All these aspect call for an efficiency optimized control techniques. Indeed, it should be noted that classical induction motor control techniques, such as vector control are not sufficient to achieve this requirement. Therefore, control techniques that maximize the induction motor efficiency are highly desirable for the fault-tolerant controller (Bose *et al.*, 1997; Haddoun *et al.*, 2005).

This paper describes an active fault-tolerant control system for a high performance induction motor drive that propels EVs or HEVs. The proposed system adaptively reorganizes itself in the event of sensor loss or sensor recovery to sustain the best control performance given the complement of remaining sensors. Moreover, the developed system takes into account the controller transition smoothness in terms of speed and torque transients. For automotive application purposes two control techniques have been chosen to illustrate the consistency of the proposed approach: *sliding mode* for encoder-based control and *fuzzy logics* for sensorless control. The system control reorganization is managed by a fuzzy decision system that assures smooth transition from the encoder-based controller to the sensorless controller and back to the encoder-based controller. Simulations tests, in terms of speed and torque responses, have been carried out on a 4-kW induction motor to evaluate the consistency and the performance of the proposed fault-tolerant control approach.

2. SLIDING MODE CONTROL

2.1. The Induction Motor Model

In a fixed *a-b* frame an induction motor can described by

$$\begin{cases} \dot{x}_1 = \gamma x_1 + \dfrac{K_L}{T_r} x_3 + n_p K_L x_4 x_5 + \alpha U_a \\ \dot{x}_2 = \gamma x_2 + \dfrac{K_L}{T_r} x_4 - n_p K_L x_3 x_5 + \alpha U_b \\ \dot{x}_3 = \dfrac{M}{T_r} x_1 - \dfrac{1}{T_r} x_3 - n_p x_4 x_5 \\ \dot{x}_4 = \dfrac{M}{T_r} x_2 - \dfrac{1}{T_r} x_4 + n_p x_3 x_5 \\ \dot{x}_5 = \beta\left(x_2 x_3 - x_1 x_4\right) - \dfrac{T_L}{J} \end{cases} \tag{1}$$

Where the stator voltages and the states are:

$$\begin{cases} U_s^T = \left[U_a \;\; U_b\right] \\ X^T = \left[x_1 \;\; x_2 \;\; x_3 \;\; x_4 \;\; x_5\right] = \left[I_{sa} \;\; I_{sb} \;\; \phi_{ra} \;\; \phi_{rb} \;\; \Omega\right] \end{cases} \tag{2}$$

2.2. Sliding Mode Control

The sliding mode control of an induction motor consists of two steps: 1) To design an equilibrium surface S such that the state trajectories of the plant restricted to the equilibrium surface have a desired behavior, such as tracking, regulation, and stability. 2) To determine a switching control law U that is able to drive the state trajectory to the equilibrium surface and maintain it on the surface. *In the proposed fault-tolerant approach, our goal is to control the speed and the rotor flux magnitude through the generation of switching controls.*

2.2.1. Switching surfaces selection

The objective consists of constructing a switched control $U_s = [U_a\ U_b]^T$ to drive the motor states to the properly designed surface $S = [S_1\ S_2]^T$ (Benchaïb *et al.*, 1999). The surfaces are defined by:

$$\begin{cases} S_1 = \frac{g_1}{\beta}\left(x_5 - \Omega_{ref}\right) + \left(x_2x_3 - x_1x_4\right) - \frac{T_L}{J\beta} - \frac{\dot{\Omega}_{ref}}{\beta} \\ S_2 = \frac{T_r}{2} g_2\left(\phi_r - \phi_{ref}\right) + \left[M\left(x_1x_3 + x_2x_4\right) - \phi_r\right] - \dot{\phi}_{ref}\frac{T_r}{2} \end{cases} \tag{3}$$

Where g_1, $g_2 > 0$. For $S \equiv 0$, we have:

$$\begin{cases} \beta\left(x_2x_3 - x_1x_4\right) - \frac{T_L}{J} = -g_1\left(x_5 - \Omega_{ref}\right) + \dot{\Omega}_{ref} \\ \frac{2}{T_r}\left[M\left(x_1x_3 + x_2x_4\right) - \phi_r\right] = -g_2\left(\phi_r - \phi_{ref}\right) + \dot{\phi}_{ref} \end{cases}$$

Using (1), we obtain:
$$\begin{cases} \dot{x}_5 = \beta\left(x_2x_3 - x_1x_4\right) - \frac{T_L}{J} \\ \dot{\phi}_r = \frac{2}{T_r}\left[M\left(x_1x_3 + x_2x_4\right) - \phi_r\right] \end{cases}$$

Then:
$$\begin{cases} \dot{x}_5 = -g_1\left(x_5 - \Omega_{ref}\right) + \dot{\Omega}_{ref} \\ \dot{\phi}_r = -g_2\left(\phi_r - \phi_{ref}\right) + \dot{\phi}_{ref} \end{cases}$$

That is:
$$\begin{cases} \frac{d}{dt}\left(x_5 - \Omega_{ref}\right) = -g_1\left(x_5 - \Omega_{ref}\right) \\ \frac{d}{dt}\left(\phi_r - \phi_{ref}\right) = -g_2\left(\phi_r - \phi_{ref}\right) \end{cases}$$

The above equation proves that for $S \equiv 0$, the rotor speed and flux magnitude square will converge exponentially to their references. Hence, to track Ω_{ref} and ϕ_{ref}, it is sufficient to make the sliding surface S attractive and invariant (Benchaïb *et al.*, 1999).

2.2.2. Switching functions synthesis

Using (1) and (3), the control law is defined by:

$$U_s = U_E + U_R \tag{4}$$

With $U_E = -A^{-1}\begin{bmatrix} U_{p1} & 0 \\ 0 & U_{p2} \end{bmatrix}\begin{bmatrix} sign(S_1) \\ sign(S_2) \end{bmatrix}$ and $U_R = -A^{-1}B$

Where $A = \begin{bmatrix} \alpha x_4 & \alpha x_3 \\ \alpha M x_3 & \alpha M x_4 \end{bmatrix}$, $B = \begin{bmatrix} f_1 \\ f_2 \end{bmatrix}$

$$S\dot{S} < 0 \Leftrightarrow \begin{cases} U_{p1} > |f_1| \\ U_{p2} > |f_2| \end{cases},\ sign(S_i) = \begin{cases} +1,\ S_i > 0 \\ -1,\ S_i < 0 \end{cases}$$

$$f_1 = \left(g_1 - \frac{1}{T_r} - \gamma\right)a_2 - g_1\frac{T_L}{\beta J} - n_p x_5\left(a_1 + K_L\phi_r\right) - \frac{g_1}{\beta}\dot{\Omega}_{ref} - \frac{1}{\beta}\ddot{\Omega}_{ref}$$

$$f_2 = \left(\frac{T_r g_2}{2} - 1\right)\dot{\phi}_r + M\left(\frac{M}{T_r}c - \left(\frac{1}{T_r} + \gamma\right)a_1 + \frac{K_L}{T_r}\phi_r + n_p x_5 a_2\right) - \frac{T_r}{2}g_2\dot{\phi}_{ref} - \frac{T_r}{2}\ddot{\phi}_{ref}$$

$$\begin{cases} a_1 = x_1x_3 + x_2x_4 \\ a_2 = x_2x_3 - x_1x_4 \\ c = x_1^2 + x_2^2 \end{cases}$$

Then, S is attractive and invariant.

2.3. Robust Flux Observer

In this study, we assume that the only measured output variables are the stator currents and the rotor speed. From (1), the rotor flux can be defined by:

$$T_r\dot{\bar{\phi}}_r + \left(1 - jn_p x_5 T_r\right)\bar{\phi}_r = M\bar{I}_s \tag{5}$$

Where $\bar{I}_s = x_1 + jx_2$

The stator voltage is given by:

$$\bar{U}_s = R_s\bar{I}_s + \sigma L_s\dot{\bar{I}}_s + \bar{E}_r \tag{6}$$

Where $\bar{U}_s = U_a + jU_b$ and $\bar{E}_r = M\sigma\alpha\dot{\bar{\phi}}_r$ (7)

E_r is the *back-emf* developed in the rotor circuit. We can define it by the terminal stator quantities.

$$\bar{E}_{r-meas} = \bar{U}_s - R_s\bar{I}_{s-meas} - \sigma L_s\dot{\bar{I}}_{s-meas}$$

$E_{r\text{-}meas}$ does not involve T_r and it is assumed as a reference model directly given by measurements. Substituting (6) in (7), we obtain the adjusted *back-emf*:

$$\bar{E}_{r-adj} = \left(1-\sigma\right)L_s\left[\frac{\bar{I}_s}{T_r} - \left(\frac{1}{T_r} - jn_p x_5\right)\frac{\bar{\phi}_r}{M}\right]$$

Therefore, rotor time constant can be estimated using *back-emf* error. Using (8), T_r can be estimated by:

$$\frac{1}{T_r} = \int \varepsilon dt = \int \left| \bar{E}_{r-meas} \times \bar{E}_{r-adj} \right| dt \tag{8}$$

Where × symbol denotes the vector cross product.

2.4. Tests of the SMC Controller

Numerical simulations have been carried out, on a 4-kW induction motor drive which ratings are summarized in the appendix, to analyze the sliding mode control performance with the rotor flux observer; before using it within the fault-tolerant controller. Speed and rotor flux corresponding to SMC, with a change in the speed reference, are shown in Figure 1.

3. FUZZY OPTIMAL VOLTS/HERTZ CONTROL

In conventional drive systems, the induction motor is driven under the open loop constant Volts/Hertz control.

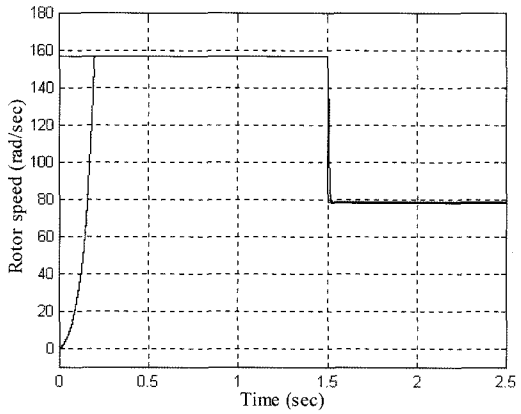

(a) Rotor speed

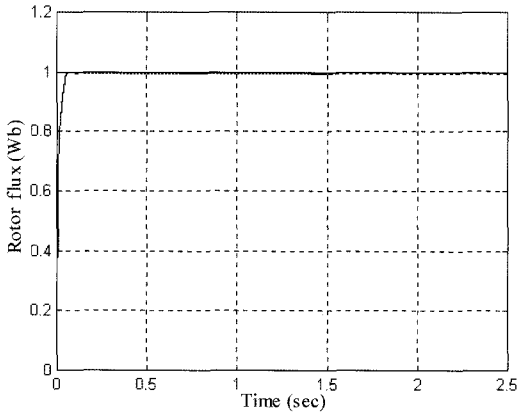

(b) Rotor flux

Figure 1. SMC performance with a change in the speed reference.

The machine flux cannot be maintained to its constant value if the stator voltage and frequency approach zero in low speed range. When the stator voltage approaches zero, it will be absorbed by the stator resistance, reducing air-gap flux, and consequently the developed torque. To overcome this problem, an optimal Volts/Hertz characteristic based on fuzzy logics is proposed to generate the voltage boost U_{bst} (Zidani *et al.*, 2001).

3.1. Volts/Hertz Control

In this section a sensorless fuzzy control technique is presented. Figure 2 illustrates its principle.

It includes the calculation of the boost voltage U_{bst}, which is added to the Volts/Hertz law in order to compensate the stator resistance voltage drop by boosting the stator voltage for low stator frequencies. With the fuzzy logic block, the stator resistance knowledge, which varies with temperature, is not required as it was proposed in several methods. *This is an important fact for automotive applications.* In fact, an EV or HEV drive system, which requires knowledge of the motor parameters, is susceptible to detuning of primarily the motor resistances. In addition, the method does not include derivative computing that would amplify noises.

3.2. Basic Principle of the Fuzzy Controller

The aim of the fuzzy logic block (FVB) is to obtain the necessary U_{bst} voltage to respect the optimal Volts/Hertz characteristic. Its input variables are the stator current magnitude variation and the voltage error existing between the measured stator voltage and the stator voltage command U_f given by the linear Volts/Hertz law. These input variables are defined as follows:

$$\begin{cases} \Delta I_s(k) = I_s(k) - I_s(k-1) \\ \Delta U_s(k) = U_f(k) - U_s(k) \end{cases} \tag{9}$$

Where k is the data sample number.

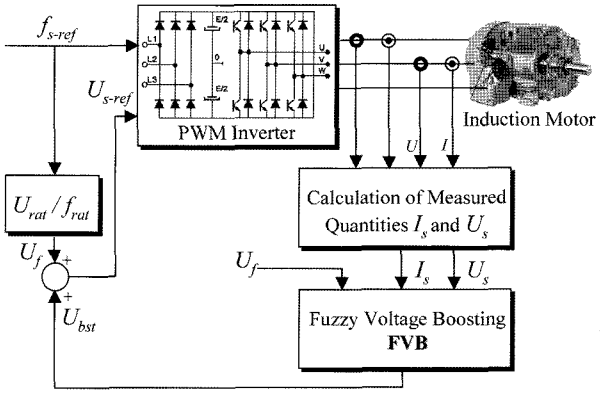

Figure 2. Sensorless fuzzy control principle.

The condition of minimum stator current requirement can be reasonably used as a rough guide to design the FVB for pursuing the optimal Volts/Hertz characteristic. The stator voltage error is used as a second input to refine the U_{bst} value.

In order to develop the fuzzy rules, simple linguistic expressions are carried out from the system knowledge and the dynamic signal analysis extracted from Figure 3 that describes the stator current and voltage behaviors due to the stator frequency variation. The following cases are then extracted:

$$\begin{cases} a_1: & \Delta I_s < 0 \ \ and \ \ \Delta U_s \cong 0 \\ a_2: & \Delta I_s \cong 0 \ \ and \ \ \Delta U_s \cong 0 \\ a_3: & \Delta I_s > 0 \ \ and \ \ \Delta U_s \cong 0 \end{cases} \tag{10}$$

$$\begin{cases} b_1: & \Delta I_s < 0 \ \ and \ \ \Delta U_s > 0 \\ b_2: & \Delta I_s \cong 0 \ \ and \ \ \Delta U_s > 0 \\ b_3: & \Delta I_s > 0 \ \ and \ \ \Delta U_s > 0 \end{cases} \tag{11}$$

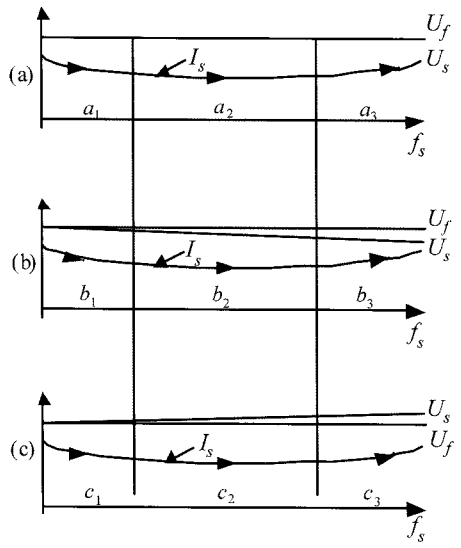

Figure 3. Stator current and voltage changes due to the stator frequency variation.

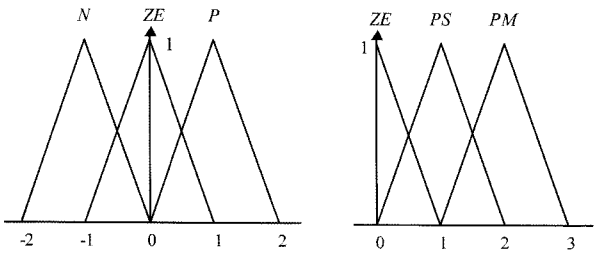

(a) Input variables ΔI_s and ΔU_s (b) Output variable U_{bst}

Figure 4. FVB membership functions.

Table 1. Linguistic control rule of the fuzzy voltage boosting.

ΔI_s \ ΔU_s	N		ZE		P	
N	ZE	c_1	PS	a_1	PM	b_1
ZE	PS	c_2	PM	a_2	PS	b_2
P	ZE	c_3	ZE	a_3	ZE	b_3

$$\begin{cases} c_1: & \Delta I_s < 0 \ \ and \ \ \Delta U_s < 0 \\ c_2: & \Delta I_s \cong 0 \ \ and \ \ \Delta U_s < 0 \\ c_3: & \Delta I_s > 0 \ \ and \ \ \Delta U_s < 0 \end{cases} \tag{12}$$

3.3. Design of the Fuzzy Voltage Boosting Block

For the FVB design, input-output variables are quantified with a suitable number of fuzzy sets. Simple triangular membership functions have been selected for all variables as shown in Figure 4. The Max-Min inference algorithm and the centroid defuzzification approach are selected to perform the last steps of the fuzzy procedure. According to the above study, Table 1 lists the carried out linguistic control rules.

3.4. Tests of the Fuzzy Controller

Numerical simulations have been carried out, on the same 4-kW induction motor drive, to analyze the performance of the sensorless fuzzy controller that will be used within the fault-tolerant controller. As shown by Figure 5, the starting torque is greatly improved; increasing the vehicle drive capabilities in the low speed region.

Furthermore, the proposed sensorless fuzzy controller meets the EVs or HEVs requirement for optimizing (maximizing) the induction motor efficiency. In fact, the

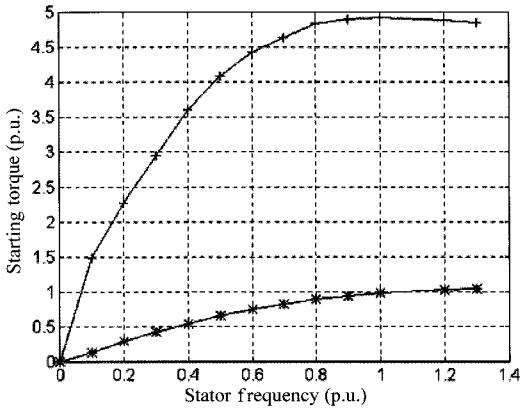

Figure 5. Starting torque characteristics (+ : with FVB and * : without FVB).

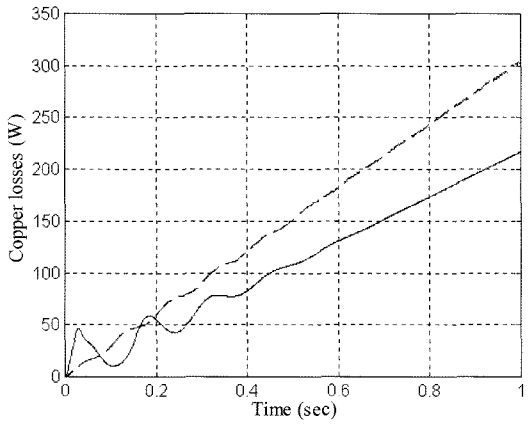

(a) 10 Hz

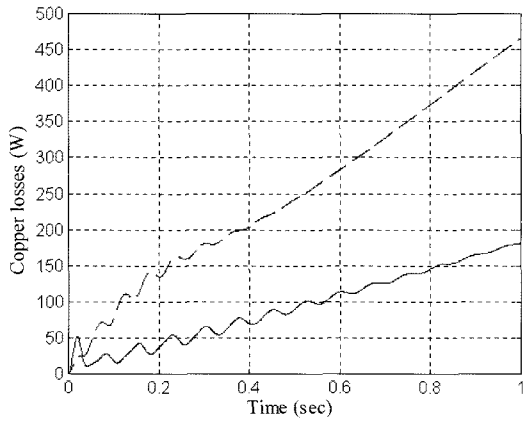

(b) 20 Hz

Figure 6. Copper losses I_s^2t (— : with FVB and - - : without FVB).

losses are minimized when the motor operated at low frequency and with rated torque as shown in Figure 6.

4. FAULT-TOLERANT CONTROL

4.1. Concept

The concept of a fault tolerant drive system is that it will continue to operate in a satisfactory manner after sustaining a fault. The term *satisfactory* implies a minimum level of performance after the fault, and will therefore be heavily influenced by system requirements (Eva Wu, 2004).

4.2. Brief Review

Many efforts have been recently devoted to study fault-tolerant control systems, namely: control systems able to detect incipient faults in sensors and/or actuators on the one hand and on the other, to promptly adapt the control law in such a way as to preserve pre-specified performances in terms of quality of the production, safety, etc. The need for these fault-tolerant systems has inspired much research for the particular case of standard three-phase induction motors (Bonivento *et al.*, 2004; Lopez-Toribio *et al.*, 2000). The majority of these contributions have been focused on faults in the drive-motor system. Where previous industrial attempts were focused on the actual drive, the current trend is to include sensors and application fault modes (Thybo, 2001; Lee and Ryu, 2003). Indeed, the overall performance of induction motor drives with a feedback structure depends not only on the health of the motor itself but also on the performance of the driving circuits and sensors: the encoder, voltage sensors, and current sensors.

For induction motor drives fault-tolerance, two control approaches have been investigated. In the first one, resilient control (also known as *accommodation*) of the drive system is adopted while retaining the same basic control strategy. In this case, the controller adapts its properties to regulate the motor output as desired by the drive system even under faults conditions (Bonivento *et al.*, 2004). In the second approach, as described in (Diallo *et al.*, 2004 and Sepe *et al.*, 2001), the control system tolerates the faults by changing the control algorithm. In this way the drive system gives degraded performance according to the faults.

4.3. Automotive Case

The high-impact nature of many electric machine applications, such as starter/alternator system in automobiles, necessitates a fault-tolerant performance. For illustration, Figure 7 shows some of the many electric machines in EVs or HEVs. For EVs and HEVs traction control, fault detection and fault-tolerance are important issues not only for the reliability of the drive system but also for the proper operation of the vehicle following a fault. Unfortunately, the automotive literature is not rich, particularly for vehicle propelled by an induction motor (Sepe *et al.*, 2001; Bennett *et al.*, 1999).

4.4. The Proposed Fault-Tolerant Control Approach

The proposed fault-tolerant approach is based on a flexible controller architecture that maintains maximum performance in the event of sensor loss or sensor recovery in the EV or the HEV electric drive. To achieve this goal, a reorganizing controller, as illustrated by Figure 8 in case of a parallel HEV, will adopt the best control methodology according to the available feedback and operational hardware.

This reconfigurable controller, whose basic principle is illustrated by Figure 9, comprises two parts, failure detection and fallback strategy. While the first part monitors the status of system sensors, the latter will engage the most appropriate control strategy based on a predetermined hierarchy.

In this paper, the fault-tolerant control system firstly

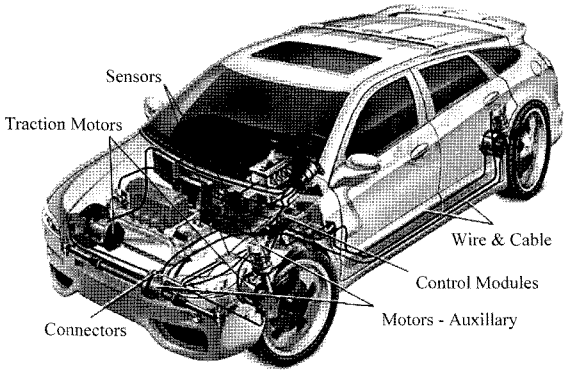

(a) Powertrain systems

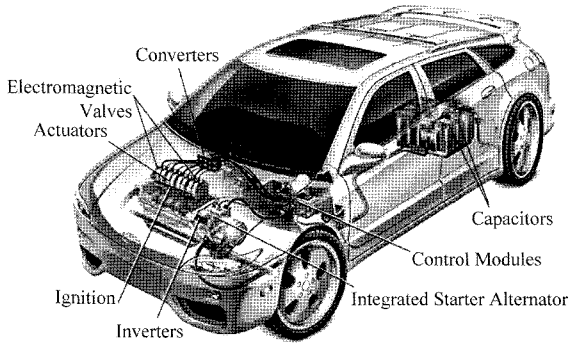

(b) By-wire systems

Figure 7. Some of the many electric machines in a HEV.

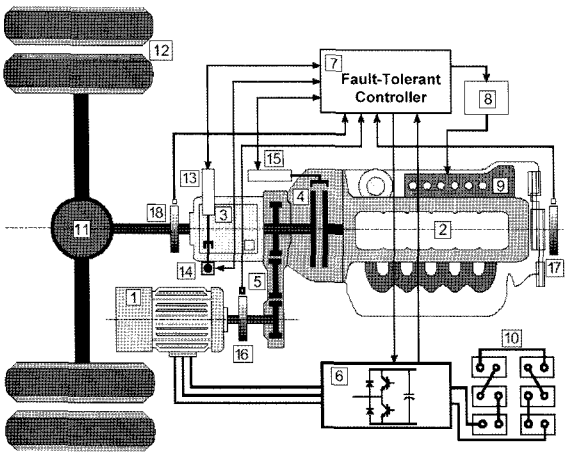

Figure 8. Schematic bloc diagram of a hybrid drive train: 1. Induction motor, 6. Inverter, 7. Fault-tolerant controller.

concerns the Sliding Mode Control (SMC) technique since better performance is obtained with an encoder to get the speed information. In the event of an unavailability of the speed sensor (e.g. failures in measurements or in the device), a sensorless fuzzy control technique or FVBC (Fuzzy Voltage Boost Control) is applied. Figure

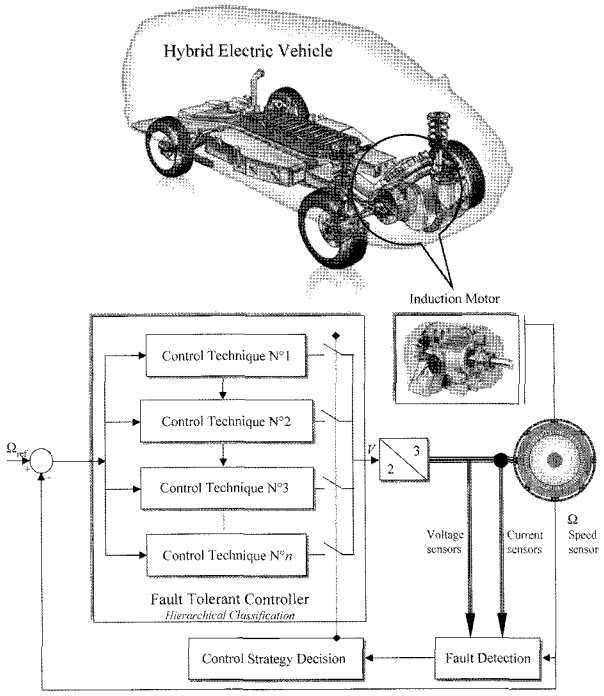

Figure 9. Overall fault-tolerant control system structure.

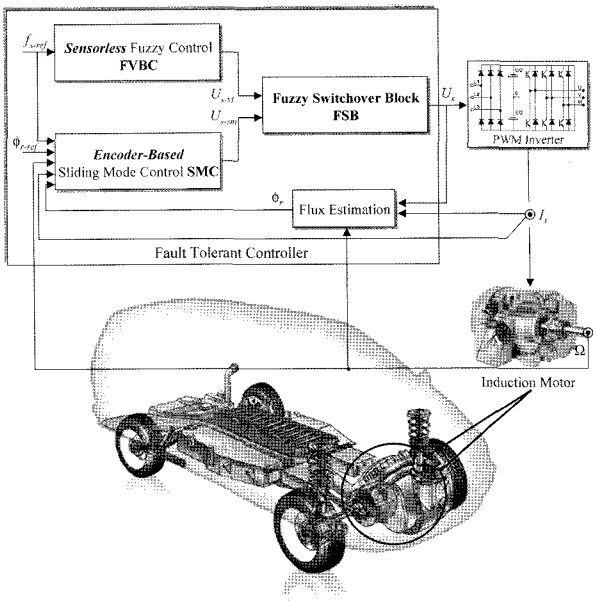

Figure 10. Fault-tolerant controller configuration.

10 shows the proposed flexible architecture for fault-tolerant control purposes.

The switchover block is based on fuzzy logic. Indeed, the controller transition that is a sensitive but complex task is better handled with a fuzzy approach.

The Fuzzy Switchover Block (FSB) consists of a fuzzification operation, a rule base, a database, and a

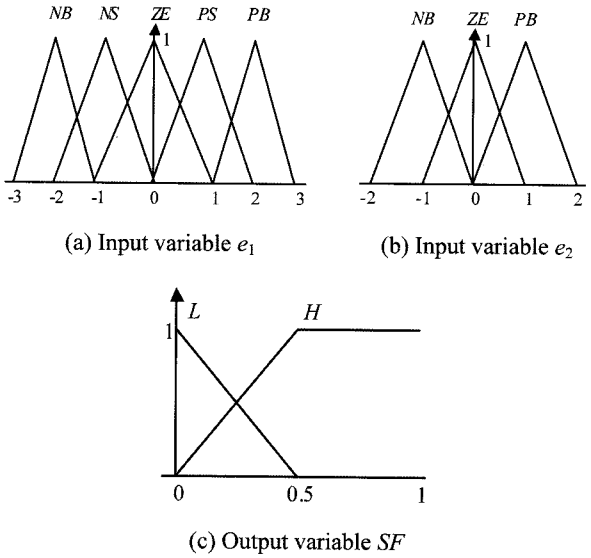

(a) Input variable e_1 (b) Input variable e_2

(c) Output variable *SF*

Figure 11. The FSB membership functions.

Table 2. Linguistic rules for the fuzzy switchover block.

e_2 \ e_1	*NB*	*NS*	*ZE*	*PS*	*PB*
NB	*H*	*H*	*H*	*H*	*H*
ZE	*L*	*L*	*H*	*L*	*L*
PB	*H*	*H*	*H*	*H*	*H*

defuzzification operation.

4.5. Controller Transition Strategy

The main idea of the FSB is to generate the suitable law U_s in order to compensate for the existing drift between $U_{s\text{-}sm}$ and U_{s_vf} (transition from SMC to FVBC) by providing a short transition between both controllers. The suitable laws U_s can be written as:

$$\bar{U}_s = f\left(\bar{U}_{s-vf}, \bar{U}_{s\text{-}sm}\right) = (1-SF)\bar{U}_{s-vf} + SF\bar{U}_{s\text{-}sm} \tag{13}$$

Where U_{s_vf} is the stator voltage generated by the FVBC; $U_{s\text{-}sm}$ is the stator voltage generated by the SMC; and *SF* is the switching function.

4.5.1. Fuzzy database

The fuzzy switchover law has the internal structure of an expert system. It samples error signals DW and DI_s at each sampling instant. Its output is the variable *SF*. The FSB inputs are defined by:

$$\begin{cases} e_1(k) = \Delta\Omega(k) = \Omega_{ref}(k) - \Omega(k) \\ e_2(k) = \Delta I_s(k) = I_s(k) - I_s(k-1) \end{cases} \tag{14}$$

Figure 11 illustrates the fuzzy subsets and the corresponding membership functions describing the input-output variables.

4.5.2. Fuzzy rules base

Knowledge is extracted in terms of *if-then* fuzzy rules. The list of the extracted rules is given in Table 2. The rules are observed to be in agreement with the system knowledge. They are consistent with our expectations. In the following, some of these rules are analyzed for illustration.

Example 1: *If* {e_1 is *PB* or *NB* "acceleration/ deceleration" and e_2 is *PB* or *NB* "induction motor drive starting mode"} *then* {*SF* must be *H* in order to favor the SMC starting mode}.

Example 2: *If* {e_1 is *PB* or *NB* "in steady state mode" and e_2 is *ZE*} *then* {*SF* is *L*}. This situation corresponds to a transition from an encoder-based control (SMC) to a sensorless control (FVBC). When the open loop Volts/ Hertz law is used, the induction machine operates with the actual operation point determinate by the load. The

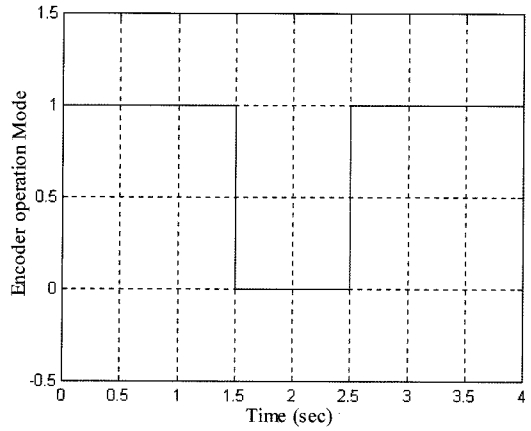

Figure 12. Transitions from SMC to FVBC and back to SMC: Encoder operation mode.

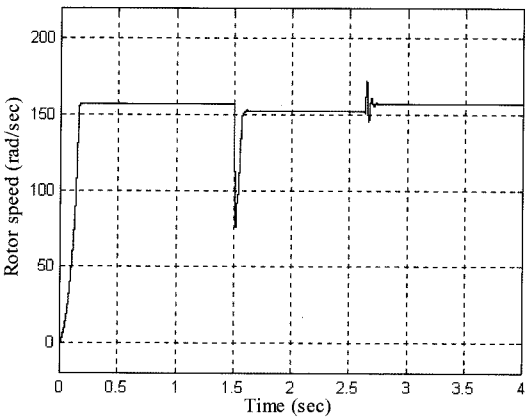

Figure 13. Transitions from SMC to FVBC and back to SMC: Rotor speed.

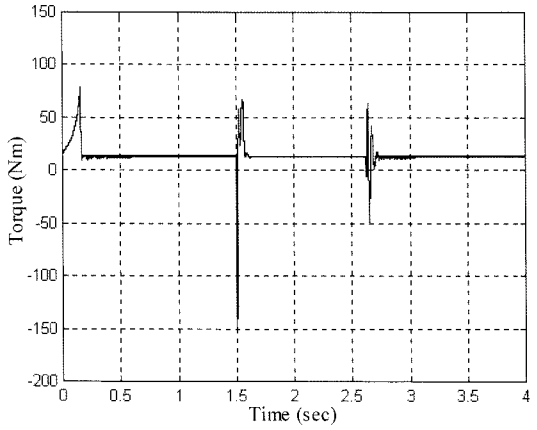

Figure 14. Transitions from SMC to FVBC and back to SMC: Torque.

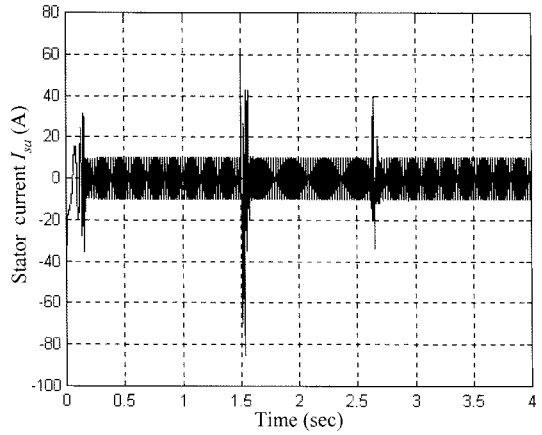

Figure 15. Transitions from SMC to FVBC and back to SMC: Stator current.

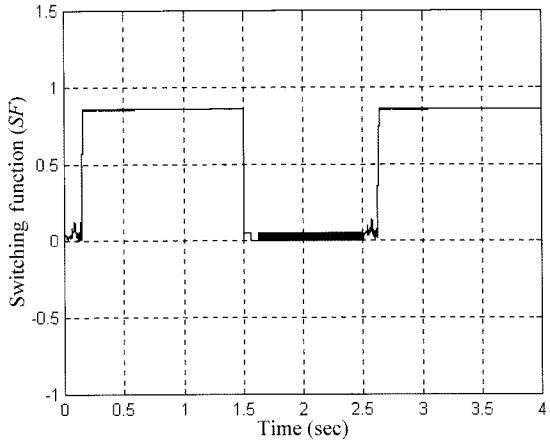

(a)

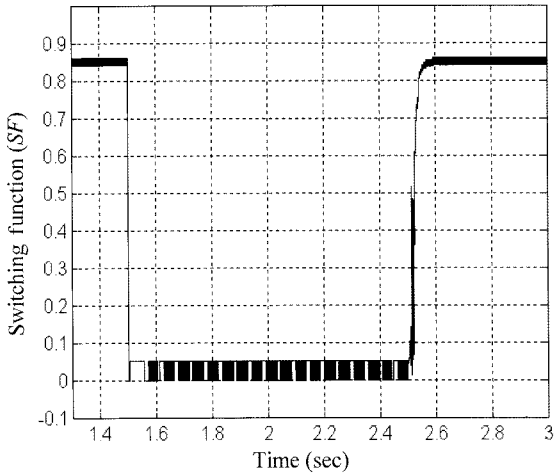

(b) Zoom

Figure 16. Transitions from SMC to FVBC and back to SMC: Switching function.

fuzzy combination law (13) leads to compensate the speed drifts when scalar control is engaged.

Example 3: *If* {e_1 is *PS* or *NS* and e_2 is *NG* or *PG* "transition from FVBC to SMC"} *then* {*SF* must be *H* to select the SMC mode}. The advantage of (13) is the possibility to have a fast transition.

Example 4: *If* {e_1 is *PS* or *NS* and e_2 is *ZE*} *then* {*SF* is *L*}. The extracted rule suggests transiting to FVBC if there is a speed variation without current variation (no load change).

Remark—We can see that some cases presented in Table 2 are not concerned by fault-tolerant operation. In this situation, the sliding mode control technique is selected since it has been proven to offer the best transient and steady state performance over the entire speed range. To be well sure that the change of variables inputs is only due to encoder anomalies, the fuzzy switchover block is activated only in steady state by detecting the variation rate of the torque current I_{sq} since the problem of parameters variation is solved.

4.6. Simulation Results

The proposed fault-tolerant control strategy has been simulated on the above mentioned 4-kW induction motor drive. Figure 12 shows the controller transition from encoder-based control (SMC) to sensorless control (FVBC) and back to encoder-based control.

At t = 1.5 sec a disturbance in the form of missing encoder pulses is introduced. Note that the rotor speed begins to decrease (Figure 13). Therefore, the FSB reconfigures the control from SMC to the sensorless FVBC. The FVBC restores then the correct system performance. This is preceded by a short torque transition as illustrated by Figure 14. At t = 2.5 sec, the encoder failure is removed. Therefore, the FSB switch back to the SMC (encoder-based control). A small torque transition is observed (Figure 14) with a variation in the stator

current as shown in Figure 15. The main function of the FSB is to provide a short and smooth transition between both SMC and FVBC controllers.

According to previous works (Sepe *et al.*, 2001) then (Diallo *et al.*, 2004) where only one controller is engaged, the proposed fuzzy transition strategy allows contributions from two neighbor controllers as it was expected, using (13), and as it is shown by Figure 16(b) that is a zoom on Figure 16(a).

5. CONCLUDING REMARKS

This paper has described an active fuzzy fault-tolerant control system for a high performance induction motor drive that propels an EV or a HEV. The proposed system adaptively reorganizes itself in the event of sensor loss or sensor recovery using a fuzzy decision system to sustain the best control performance given the complement of remaining sensors. Moreover, this fuzzy system manages the controller transition smoothness in terms of speed and torque transients.

For automotive application purposes two control techniques have been chosen to illustrate the consistency of the proposed approach, the sliding mode for encoder-based control and the fuzzy logics for sensorless control. The sliding mode control technique has been selected since it is one of the effective nonlinear robust control approaches since it provides system dynamics with an invariant property to uncertainties. Moreover, it has been proven to offer the best transient and steady state performance over the entire speed range. The sensorless fuzzy control has been selected since it is effective at handling the uncertainties and nonlinearities associated with complex control systems such as traction control. Moreover, the proposed fuzzy control approach has two main features that meet with automotive applications requirements: a) the stator resistance knowledge, which varies with temperature, is not required as it was the case in several methods; b) optimization (maximization) of the traction induction motor efficiency.

Simulations tests have been carried out on a 4-kW induction motor drive. The obtained results show that the proposed fault-tolerant approach provides a simple configuration but with high performance in term of speed and torque responses. Moreover, it has been shown the global consistency and effectiveness of the fault-tolerant control strategy in comparison to previous studies (Sepe *et al.*, 2001), even with other type of electric propulsion (Jeong *et al.*, 2005; Parsa and Toliyat, 2003; Mir *et al.*, 2004).

REFERENCES

Benchaïb, A., Rachid, A., Audrezet, E. and Tadjine, M. (1999). Real-time sliding mode observer and control of induction motor. *IEEE Trans. Industrial Electronics* **46**, 1, 128–138.

Bennett, S. M., Patton, R. J. and Daley, S. (1999). Sensor fault-tolerant control of a rail traction drive. *Control Engineering Practice*, **7**, 217–225.

Bonivento, C., Isidori, A., Marconi, L. and Paoli, A. (2004). Implicit fault-tolerant control: Application to induction motors. *Automatica*, **40**, 355–371.

Bose, B. K., Patel, N. R. and Rajashekara, K. (1997). A neuro-fuzzy-based on-line efficiency optimization control of a stator flux-oriented direct vector-controlled induction motor drive. *IEEE Trans. Industrial Electronics* **44**, **2**, 270–273.

Chan, C. C. (2002). The state of the art of electric and hybrid vehicles. *Proc. IEEE* **90**, **2**, 247–275.

Chan, C. C., Leung, W. S. and Ng, C. W. (1990). Adaptive decoupling control of induction motor drives. *IEEE Trans. Industrial Electronics* **37**, **1**, 41–47.

Chen, H., Zhang, D. and Guo, Y. (2001). A novel green electric drive system. *Proc. 2001 IEEE ICSMC*, **5**, 3157–3162.

Chen, Z. and Liu, L. (2003). Neural networks based electric motor drive for transportation systems. *Proc. 2003 IEEE ITS*, **2**, 1378–1383.

De Rossier Corrêa, M. B., Jacobina, C. B., Da Silva, E. R. C. and Lima, A. N. (2001). An induction motor drive system with improved fault tolerance. *IEEE Trans. Industry Applications* **37**, **5**, 873–879.

Diallo, D., Benbouzid, M. E. H. and Makouf, A. (2004). A fault-tolerant control architecture for induction motor drives in automotive applications. *IEEE Trans. Vehicular Technology* **53**, **6**, 1847–1855.

Eva Wu, N. (2004). Coverage in fault-tolerant control. *Automatica*, **40**, 537–548.

Faiz, J., Sharifian, M. B. B., Keyhani, A. and Proca, A. B. (2003). Sensorless direct torque control of induction motors used in electric vehicle. *IEEE Trans. Energy Conversion* **18**, **1**, 1–10.

Haddoun, A., Benbouzid, M. E. H. and Diallo, D. (2005). A loss-minimization DTC scheme for EV induction motors. *Proc. 2005 IEEE VPPC*, 315–321.

Jeong, Y. S., Sul, S. K., Schulz, S. E. and Patel, N. R. (2005). Fault detection and fault-tolerant control of interior permanent-magnet motor drive system for electric vehicle. *IEEE Trans. Industry Applications* **41**, **1**, 46–51.

Klima, J. (2003). Analytical investigation of an induction motor drive under inverter fault mode operations. *IEE Proc.-Electric Power Applications* **150**, **3**, 255–262.

Lascu, C. and Trzynadlowski, A. M. (2004). A sensorless hybrid DTC drive for high-volume low-cost applications. *IEEE Trans. Industrial Electronics* **51**, **5**, 1048–1055.

Lee, H. D. and Sul, S. K. (1998). Fuzzy-logic-based

torque control strategy for parallel-type hybrid electric vehicle. *IEEE Trans. Industrial Electronics* **45**, **4**, 625–632.

Lee, K. S. and Ryu, J. S. (2003). Instrument fault detection and compensation scheme for direct torque controlled induction motor drives. *IEE Proc.-Control Theory Applications* **150**, **4**, 376–382.

Lopez-Toribio, J. C., Patton, R. J. and Daley, S. (2000). Takagi–Sugeno fuzzy fault-tolerant control of an induction motor. *Neural Computing & Applications*, **9**, 19–28.

Mir, S., Islam, M. S., Sebastian, T. and Husain, I. (2004). Fault-tolerant switched reluctance motor drive using adaptive fuzzy logic controller. *IEEE Trans. Power Electronics* **19**, **2**, 289–295.

Mutoh, N., Kaneko, S., Miyazaki, T., Masaki, R. and Obara, S. (1997). A torque controller suitable for electric vehicles. *IEEE Trans. Industrial Electronics* **44**, **1**, 54–63.

Neacsu, D. O. and Rajashekara, K. (2001). Comparative analysis of torque-controlled IM drives with applications in electric and hybrid vehicles vehicle. *IEEE Trans. Power Electronics* **16**, **2**, 240–247.

Parsa, L. and Toliyat, H. A. (2003). A self reconfigurable electric motor controller for hybrid electric vehicle applications. *Proc. 2003 IEEE IECON*, **1**, 919–924.

Proca, A. B., Keyhani, A. and Miller, J. M. (2003). Sensorless sliding-mode control of induction motors using operating condition dependent models. *IEEE Trans. Energy Conversion* **18**, **2**, 205–212.

Rahman, Z., Ehsani, M. and Butler, K. L. (2000). An investigation of electric motor drive characteristics for EV and HEV propulsion systems. *SAE Paper No.* 2000-01-3062.

Sepe, R. B., Fahmi, B., Morrison, C. and Miller, J. M. (2001). Fault tolerant operation of induction motor drives with automatic controller reconfiguration. *Proc. 2001 IEEE IEMDC*, 156–162.

Ta, C. M. and Hori, Y. (2001). Convergence improvement of efficiency-optimization control of induction motor drives. *IEEE Trans. Industry Applications* **37**, **6**, 1746–1754.

Thybo, C. (2001). Fault-tolerant control of induction motor drive applications. *Proc. 2001 IEEE ACC*, **4**, 2621–2622.

Zeraoulia, M., Benbouzid, M. E. H. and Diallo, D. (2005). Electric motor drive selection issues for HEV propulsion systems: A comparative study. *Proc. 2005 IEEE VPPC*, 280–287.

Zidani, F., Naït-Saïd, M. S., Diallo, D. and Benbouzid, M. E. H. (2001). Fuzzy optimal Volts/Hertz control method for an induction motor. *Proc. 2001 IEEE IEMDC*, 377–381.

APPENDIX

Rated data of the simulated induction motor

Rated values	Power	4	kW
Frequency		50	Hz
	Voltage (Δ/Y)	220/380	V
	Current (Δ/Y)	15/8.6	A
	Speed	1440	rpm
	Pole pair (n_p)	2	
	Power factor	0.8	
Rated parameters	R_s	1.150	Ω
	R_r	1.440	Ω
	L_s	0.156	H
	L_r	0.156	H
	M	0.143	H
Constants	J	0.024	kg.m^2
	f	0.011	IS